ACS APPLIED MATERIALS & INTERFACES

Letter

www.acsami.org

Interface-Located Photothermoelectric Effect of Organic Thermoelectric Materials in Enabling NIR Detection

Dazhen Huang,[†,‡] Ye Zou,[‡] Fei Jiao,[†,‡] Fengjiao Zhang,[†,‡] Yaping Zang,[†,‡] Chong-an Di,*[,†] Wei Xu,*[,†] and Daoben Zhu*[,†]

[†]Beijing National Laboratory for Molecular Sciences, Key Laboratory of Organic Solids, Institute of Chemistry, Chinese Academy of Sciences, Beijing 100190, P. R. China

[‡]University of Chinese Academy of Sciences, Beijing 100049, P. R. China

Supporting Information

ABSTRACT: Organic photothermoelectric (PTE) materials are promising candidates for various photodetection applications. Herein, we report on poly[Cu_x(Cu-ett)]:PVDF, which is an excellent polymeric thermoelectric composite, possesses unprecedented PTE properties. The NIR light irradiation on the poly[Cu_x(Cu-ett)]:PVDF film could induce obvious enhancement in Seebeck coefficient from 52 ± 1.5 to 79 ± 5.0 μV/K. By taking advantage of prominent photothermoelectric effect of poly[Cu_x(Cu-ett)]:PVDF, an unprecedented voltage of 12 mV was obtained. This excellent performance enables its promising applications in electricity generation from solar energy and NIR detection to a wide range of light intensities ranging from 1.7 mW/cm^2 to 17 W/cm^2.

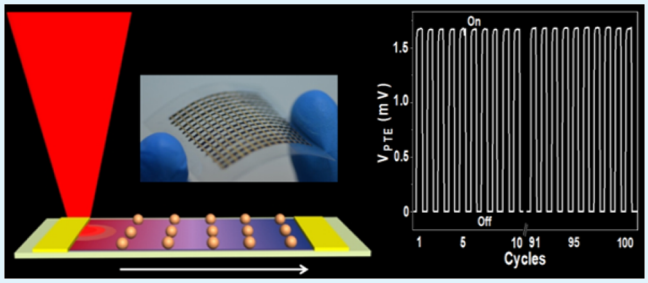

KEYWORDS: *photothermoelectric effect, NIR detection, organic thermoelectric material, organic thermoelectric device*

By virtue of intrinsically low thermal conductivity and potentially ultralow cost, organic thermoelectric materials are now considered to be attractive thermoelectric candidates and have attracted increasing attention in the past few years.[1−5] Recently, great achievements have been made in organic thermoelectric materials and devices, as indicated by dramatically improved thermoelectric performance.[6−12] For instance, by implementing chemical doping of poly(3,4-ethylenedioxythiophene) (PEDOT) with poly(styrenesulfonate), an unprecedented figure-of-merit (ZT) value of 0.42 has been achieved.[12] Moreover, we have previously demonstrated that an 1,1,2,2-ethenetetrathiolate(ett)-metal coordination polymer, poly[K_x(Ni-ett)], which is an n-type thermoelectric material, exhibits a high ZT value of 0.2.[11] These promising performances, along with the unique features of organic thermoelectric materials in flexibility, demonstrate the great potential of organic materials in various thermoelectric applications.

Light irradiation on thermoelectric materials generally affects thermoelectric conversion by means of the photothermoelectric (PTE) effect, which can be further classified into both photo-thermoelectric (P-T-E) and photo-thermoelectric (P-TE) effects. For the P-T-E effect, light energy is transferred into electricity via a combination of typical photothermal and thermoelectric effects. Incorporating the P-T-E effect of a selenophene derivative (hexyl-3,4-ethyl-enedioxyselenophene, EDOS-C6) with near-infrared (NIR) irradiation, a significant temperature gradient (ΔT) across PEDOS-C6 can be established, leading to the generation of a high Seebeck voltage of up to 900 μV under moderate NIR light exposure (808 nm @ 2.33 W/cm^2).[13] In addition to the P-T-E conversion, photoinduced excitation of the organic active materials can also occur, with an obvious influence on the thermoelectric properties. The so-called P-TE effect has been evidenced by an example based on poly(2-methoxy-5-(2′-ethylhexyloxy)-p-phenylenevinylene) (MEH-PPV). It was observed that photo-excitation-generated excited states of MEH-PPV contribute to an obvious increase in thermoelectric performance, including enhancement in both the Seebeck coefficient and electrical conductivity (σ).[14] These results imply that the light irradiation can not only serve as a power source for energy conversion by thermoelectric materials via a typical P-T-E effect but also might be utilized to improve thermoelectric performance via the P-TE effect.

Benefiting from the efficient conversion of photons to an electric signal, active materials with prominent PTE properties such as graphene and MoS_2 are believed to be promising candidates for photodetection applications.[15−22] To date, a series of photodetectors based on graphene and MoS_2 have been demonstrated.[18,19,21] In contrast with the rapid development of inorganic PTE materials and devices, few organic thermoelectric materials have been shown to exhibit PTE properties. Given that organic materials usually possess excellent flexibility and solution processability, the exploration

Received: February 13, 2015
Accepted: April 15, 2015
Published: April 15, 2015

DOI: 10.1021/acsami.5b01460
ACS Appl. Mater. Interfaces 2015, 7, 8968−8973

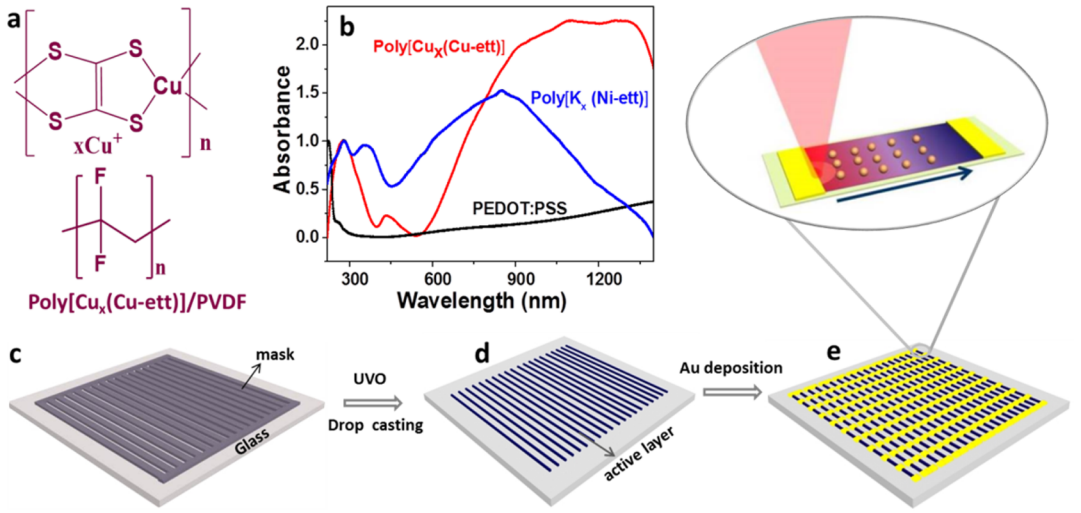

Figure 1. (a) Molecular structures of poly[Cu$_x$(Cu-ett)] and PVDF. (b) UV−vis−NIR diffuse reflectance spectra of poly[Cu$_x$(Cu-ett)], poly[K$_x$(Ni-ett)], and PEDOT:PSS. (c−e) Schematic diagram of the fabrication process of PTE devices: (c) lamination of a patterned mask was attached on the OTS-modified glass substrate, (d) deposition of patterned active layer via drop casting, (e) device geometry of fabricated PTE device.

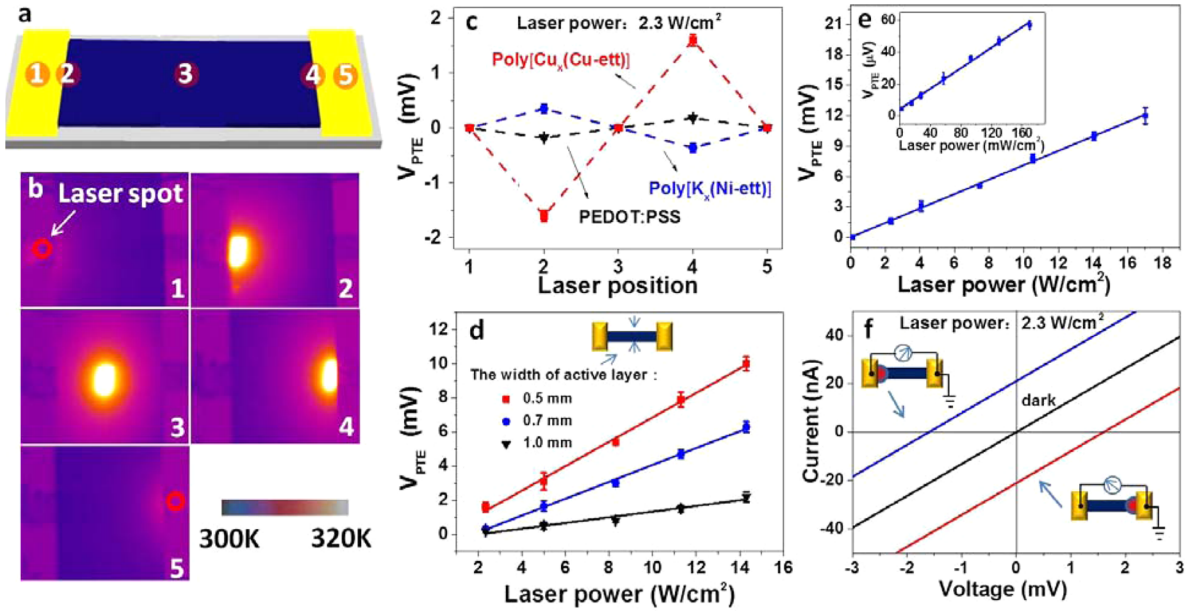

Figure 2. (a) Schematic diagram of PTE devices under laser irradiation at different positions from No. 1 to No. 5. (b) IR camera images of PTE devices upon NIR irradiation (λ = 808 nm @ 2.3 W/cm^2) at different positions marked in a. (c) Generated V_{PTE} for the different materials based devices under NIR exposure (λ = 808 nm @ 2.3 W/cm^2) at different positions marked in a. (d) Generated V_{PTE} versus laser power for the poly[Cu$_x$(Cu-ett)]:PVDF-based devices with different active layer widths. (e) NIR laser power-dependent V_{PTE} for the devices based on different materials when the laser spot is fixed at the interface between Au electrode and active layers. (f) I−V curve of poly[Cu$_x$(Cu-ett)]:PVDF composite-based devices under NIR exposure (λ = 808 nm @ 2.3 W/cm^2).

of organic PTE materials are highly desired. Herein, we demonstrate that poly[Cu$_x$(Cu-ett)], a polymeric thermoelectric material, exhibit excellent PTE properties featured by the efficient photothermal conversion as well as photoinduced enhancement of Seebeck coefficient from 52 ± 1.5 to 79 ± 5.0 μV/K. This unprecedented P-TE effect of poly[Cu$_x$(Cu-ett)], together with the electrode/organic interface-located P-T-E effect in the thermoelectric device, enables effective detection of NIR light and even allows for electricity generation toward solar energy harvesting.

The PTE properties of organic TE materials are determined by the light-thermal conversion efficiency and thermoelectric properties of the active layer, while strong light absorbance is a prerequisite for prominent PTE materials. Figure 1b shows the UV−vis−NIR diffuse reflectance spectrum of the poly[Cu$_x$(Cu-ett)], poly[K$_x$(Ni-ett)] and PEDOT. Given that poly[Cu$_x$(Cu-ett)] shows strong absorbance in the near NIR region (800−1400 nm) and good thermoelectric properties, it might be a promising PTE material. However, poly[Cu$_x$(Cu-ett)] suffers from a shortcoming of poor insolubility in organic solvents, which impedes the deposition of the film via solution-processing techniques. Alternatively, a solution processable composite, poly[Cu$_x$(Cu-ett)]:poly(vinylidene fluoride) (PVDF) (Figure 1a), was chosen as the active layer following a previous report (Figure S1 in the Supporting Information).[23] Figure 1c−e is a schematic diagram of the fabrication

DOI: 10.1021/acsami.5b01460
ACS Appl. Mater. Interfaces 2015, 7, 8968−8973

process of the PTE devices. The details are shown in the Supporting Information.

The PTE voltage (V_{PTE}) generation of the poly[Cu_x(Cu-ett)]:PVDF film upon NIR irradiation was investigated using a home-built system integrated with temperature monitoring system, an electrical signal measurement system and a high resolution translation stage. By scanning the device through a NIR laser (λ = 808 nm) with simultaneously recorded TE voltage, PTE measurements can be performed. It is noteworthy that the V_{PTE} of poly[Cu_x(Cu-ett)]:PVDF film can only be detected when the laser spot was moved along the electrode-active layer contact edge (position No. 2 in Figure 2a) (Figure 2a–c). Once the laser spot was located on the electrodes or on the poly[Cu_x(Cu-ett)] film between the two electrodes (positions No. 1 and No. 3 in Figure 2a), no obvious V_{PTE} was detected. However, when the NIR laser spot was moved from one electrode/organic layer interface to another (from position No. 2 to position No. 4), it led to the generation of an opposite voltage with a comparable value.

In addition to the interface-located PTE effect, the PTE performance of the device is strongly dependent on the width of the active-layer (Figure 2d). When the active layer width was maintained at 1.0 mm, a V_{PTE} of 1.9 mV was obtained (with a laser power of 14 W/cm^2). In a comparison, a voltage higher than 10 mV, which represent an improvement of over 400% in V_{PTE}, was achieved once the width was decreased to 0.5 mm (Figure 2d). This result indicated that small active layer width facilitates the enhancement of the V_{PTE}. Therefore, we can make conclusion that the electrode/organic layer interface located PTE effect, which is affected by the width of the active layer, is responsible for the large V_{PTE} generation. Moreover, the wavelength of the NIR light also affects the generated voltage. For instance, an expected smaller voltage was obtained when the wavelength was changed from 808 to 650 nm (Figure S2 in the Supporting Information), because of the weaker absorbance of the active film (Figure 1b).

Devices based on poly[K_x[Ni-ett] and PEDOT were also constructed to evaluate the applicability of the interface-located PTE effect (Figure S3 in the Supporting Information). All the devices exhibited similar interface-located PTE effect, in that the PTE voltages were only generated at the contact edge area. The poly[K_x(Ni-ett)]-based devices displayed opposite voltages in comparison with the poly[Cu_x(Cu-ett)]-based devices, owing to the n-type nature of the poly[K_x(Ni-ett)]. Although the V_{PTE} generated by the poly[K_x[Ni-ett] and PEDOT-based devices were smaller than those obtained from the poly-[Cu_x(Cu-ett)]-based devices (Figure 2c), the interface-located PTE effect can be routinely observed for different thermo-electric materials.

The dependence of V_{PTE} on the laser power was investigated in order to further analyze the PTE effect. For all the examined TE devices, the generated voltage was linearly dependent on the NIR laser power (Figure 2e and Figure S4 in the Supporting Information). By taking advantage of the high V_{PTE} generation of poly[Cu_x(Cu-ett)], an unprecedented voltage of 12 mV was obtained when the sample was irradiated by the NIR laser with a power density of 17 W/cm^2 (Figure 2e). The PTE voltage reached 1.6 mV when the laser power was maintained at 2.3 W/cm^2, which is higher than that of PEDOS-C6, the most excellent organic PTE material ever reported (0.9 mV @ 2.3 W/cm^2).[13] It should be noted that the V_{PTE} is even higher than the values of many PTE devices based on MoS_2 and graphene under the same NIR irradiation (Table 1). More importantly, we obtained a V_{PTE} of 4.5 μV once the light density decreased to 1.7 mW/cm^2 (Figure 2e). It thus indicated that the poly[Cu_x(Cu-ett)]:PVDF-based device can respond to a wide range of NIR light intensities, ranging from 1.7 mW/cm^2 to 17 W/cm^2. This sensitive response to NIR light, together with a short response time (<30 μs) (Figure S5 in the Supporting Information), make poly[Cu_x(Cu-ett)] an excellent candidate for NIR detection application.

Table 1. V_{PTE} of PTE Devices Based on Different Materials

active materials	V_{PTE}	laser power (W/cm^2)	ref
poly[Cux(Cu-ett)]: PVDF	50 μV	0.14	this work
	1.6 mV	2.3	this work
	10 mV	14.1	this work
PEDOS-C6	0.9 mV	2.33	13
MoS_2	10 mV	7600	29
graphene	0.4 mV	>10000	22

As for the PTE device, the voltage is determined by the Seebeck coefficient (S) and the light-induced temperature gradient (ΔT) across the sample ($V_{PTE} = S \times \Delta T$). Notably, the Seebeck coefficient is a key parameter in the evaluation of the TE properties, whereas the light-induced ΔT is determined by the absorbance of NIR light and the photothermal conversion efficiency of the TE materials. Both Seebeck coefficient and ΔT were measured to obtain a deeper understanding of the interface-located PTE effect on the poly[Cu_x(Cu-ett)]:PVDF composite. As a result of the strong absorbance of the NIR light and efficient photothermal conversion, a high temperature difference of up to 76.1 K was achieved at a laser power of 8.7 W/cm^2 (Figure S6 in the Supporting Information). The temperature difference across the poly[Cu_x(Cu-ett)]:PVDF composite film is obviously higher than that of the poly[K_x(Ni-ett)]:PVDF composite and PEDOT films. More importantly, an unexpected Seebeck coefficient value of 79 ± 5.0 μV/K (Table S1 in the Supporting Information), which is higher than the value of the pristine device without NIR irradiation (52 ± 1.5 μV/K), can be routinely obtained. As a comparison, no obvious increase in Seebeck coefficient was found when the poly[K_x(Ni-ett)] and PEDOT film were exposed to NIR light (Table S2 in the Supporting Information). This result demonstrates that the NIR light irradiation exerts a significant influence on the Seebeck coefficient of the poly[Cu_x(Cu-ett)]:PVDF composite.

Considering that there is a slight increase in the base temperature (from 25 to 31 °C) upon NIR irradiation at the electrode/active-layer interface with laser power ranging from 2 W/cm^2 to 17 W/cm^2, it can be concluded that the change in the base temperature was not majorly responsible for the enhancement of the Seebeck coefficient (Figure S7 in the Supporting Information). The general expression for Seebeck coefficient is[26,27]

$$S = \frac{k_B}{e}\int \frac{E_F - E}{k_B T}\frac{\sigma(E)}{\sigma}dE = -\frac{k_B}{e}\left(\ln\frac{n}{N_C} + A\right)$$

where K_B is the Boltzmann constant, e is the electron charge, E_F is the Fermi energy of the materials, $\sigma(E)$ is the electronic conductivity, T is the absolute temperature, n is the carrier concentration, and N_C is the effective density of states (DOS). Therefore, Seebeck coefficient is affected by the energy level, which is related to the carrier density as well as the DOS. For

DOI: 10.1021/acsami.5b01460
ACS Appl. Mater. Interfaces 2015, 7, 8968–8973

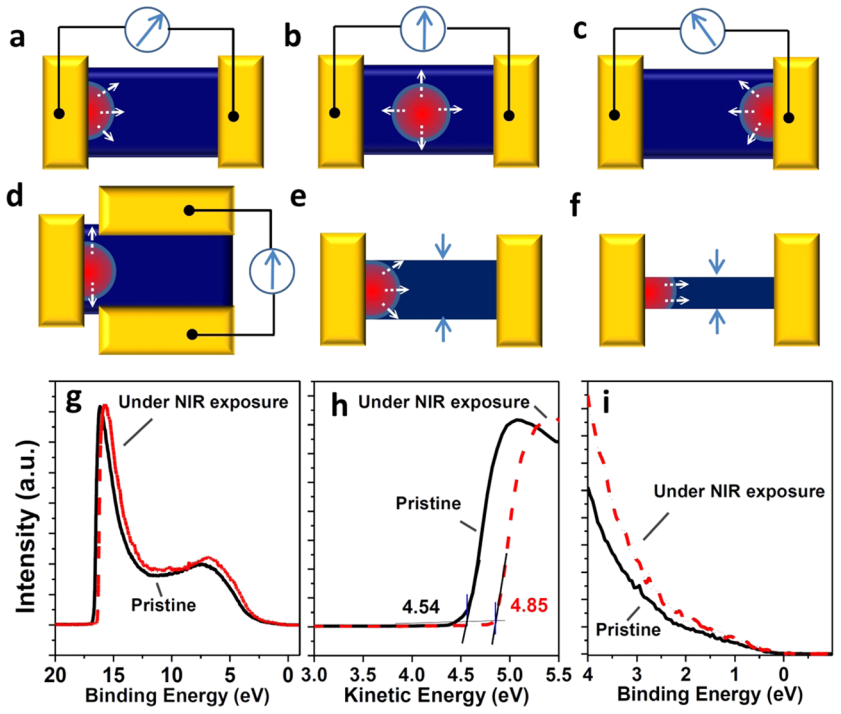

Figure 3. (a–d) Schematic diagram mechanism of NIR laser-induced interface-located photothermoelectric effect when the NIR laser is located at different positions. (e, f) Schematic diagram mechanism of active line width dependent PTE effect. (g–i) UPS spectra of poly[Cu_x(Cu-ett)] with and without NIR (808 nm) exposure.

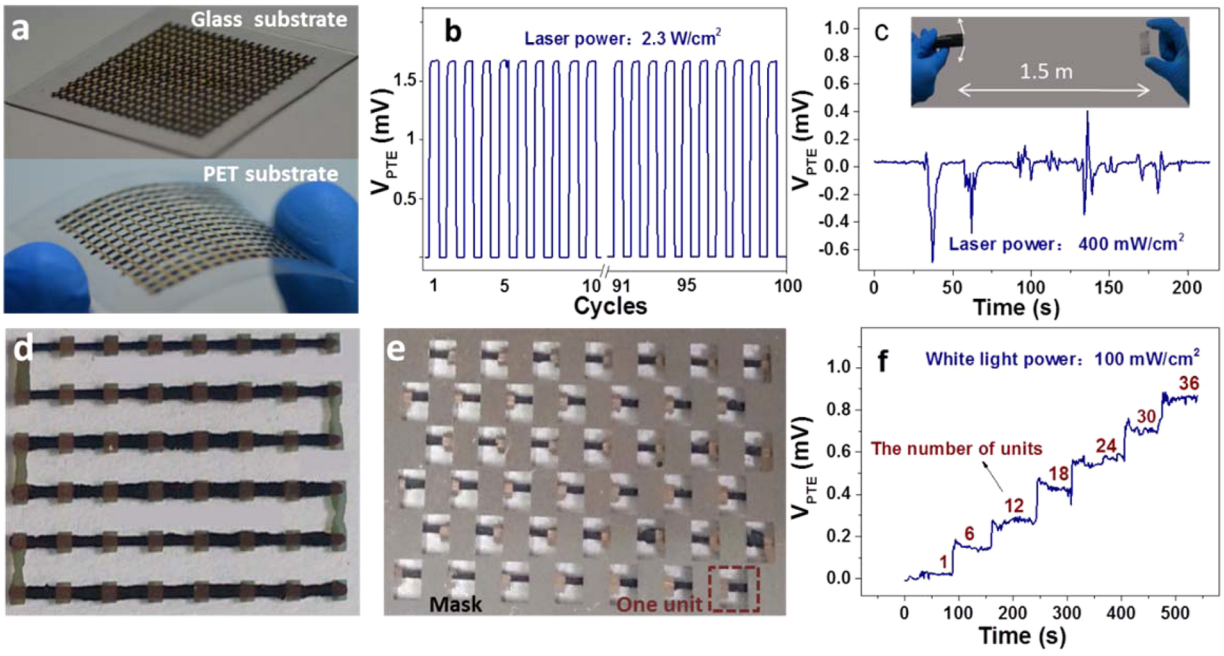

Figure 4. (a) Photo images of NIR detectors on glass and PET substrates. (b) NIR detection cyclabiility of photothermoelectric device under a laser intenstity of 2.3 W/cm^2 for 100 cycles. (c) Voltage generation of the flexible detectors when a NIR (400 mW/cm^2) laser was was moved randomly approximately 1.5 m from the integrated detector. Photo images of a integrated device for electricity generation (d) without and (e) with shadow mask. (f) Voltage generation when varied units are exposed to the sunlight.

further understanding of the light-induced enhancement of Seebeck coefficient, ultraviolet photoelectron spectroscopy (UPS) measurements were performed. From the UPS spectrum (Figure 3g–i), the poly[Cu_x(Cu-ett)] film was found to display a surface work function of 4.54 eV. However, an obvious upward vacuum level shift, which indicates an increased work function of 4.85 eV, was observed when the sample was exposed to NIR light (808 nm). This result implies that NIR irradiation on poly[Cu_x(Cu-ett)] can lead to a 0.31 eV increase in the workfunction. Moreover, the magnified view of the low-binding-energy regions shows the density of valence electronic states (DOVS) of poly[Cu_x(Cu-ett)].[28] An obvious difference in the slope of the DOVS near the Fermi level before and after NIR irradiation confirms the difference in Seebeck

DOI: 10.1021/acsami.5b01460
ACS Appl. Mater. Interfaces 2015, 7, 8968–8973

coefficient. However, only slight or even no obvious changes in workfunction were observed when the poly[K_x(Ni-ett)]- and PEDOT- based films were exposed to NIR light. It can be concluded that the prominent PTE properties of poly[Cu_x(Cu-ett)] are ascribed to existence of central Cu ions. In previous reports, the structural difference between the ground and excited states of Cu-based complexes has been reported, and is attributed to the transference of electrons from central copper ions to the ligands due to metal-to-ligand charge transfer excitation.[24,25] In this case, although the detailed investigation of the mechanism is still underway, we suspect that the light irradiation leads to a similar intramolecular charge transfer from central copper to the ligands. The photoinduced excitation of poly[Cu_x(Cu-ett)] facilitates an increase in the DOS near E_F and work function, which results in the obvious enhancement of the Seebeck coefficient.

The obtained PTE phenomenon can be understood as follows. When the electrode is irradiated by NIR light, no V_{PTE} can be generated since the gold electrode possesses high thermal conductivity and limited absorbance to the NIR light. Although NIR light can be absorbed by the poly[Cu_x(Cu-ett)] layer to create a high-temperature region when the laser spot is moved to the active layer between two electrodes, ΔT is generated in all directions (Figure 3b). Considering the unipolar transport property of the poly[Cu_x(Cu-ett)] film, V_{PTE} are generated in all directions, leading to a symmetric neutralization of the overall V_{PTE}. Therefore, no V_{PTE} is detected. By comparison, once the laser spot is maintained at the electrode/organic contact edge (Figure 3a and 3c), an asymmetric ΔT is generated on the active layer and contributes to the generation of a large ΔT. The smaller the width of the active layer, the higher the asymmetry of ΔT, and thus the higher the V_{PTE} (Figure 3e, f). In the case of a poly[Cu_x(Cu-ett)]:PVDF-based PTE device with an optimized active layer width, a large asymmetric ΔT can be generated at the electrode/active-layer interface as a result of its strong absorbance of NIR light and efficient photothermal conversion. This prominent P-T-E property, combined with the obviously enhanced Seebeck coefficient value via the P-TE effect, contribute to the generation of large V_{PTE} in poly[Cu_x(Cu-ett)]: PVDF-based devices.

By taking advantage of the outstanding PTE performance, sensitive NIR detection can be achieved. We fabricated poly[Cu_x(Cu-ett)]:PVDF composite based integrated devices on both glass and PET substrates (Figure 4a). All the devices displayed a rapid and reproducible response to NIR light irradiation. The light-induced voltages were stable over one hundred cycles of NIR switching. For example, the devices could generate a high voltage (up to 1.6 mV) upon reproducible 2.3 W/cm^2 NIR light irradiation (Figure 4b). Such convertible devices can be fabricated on PET substrates to build a flexible NIR detector. Figure 4c shows the voltage generation of flexible detectors when a NIR (400 mW/cm^2) laser was operated approximately 1.5 m from the integrated detector. The device could respond quickly, generating V_{PTE} values ranging from 0.2 to 0.6 mV when the laser was moved randomly, indicating the promising application of our devices for NIR detection. It is also worth noting that this voltage generation is much larger than that in vertical devices under the same NIR light irradiation (Figure S8 in the Supporting Information), because of the fact that a large ΔT is difficult to create using a thin film in a vertical device.

Considering the prominent PTE properties of poly[Cu_x(Cu-ett)]:PVDF composite, we also constructed an energy-generation device array to achieve solar energy harvesting. As shown in Figure 4d–f, a voltage of 25 μV could be generated when a single PTE device was exposed to simulated solar light with a power intensity of 100 mW/cm^2. Moreover, the value of V_{PTE} increased linearly with an increasing number of exposed devices, and a maximum voltage of 0.9 mV could be obtained when 36 devices were exposed to the light irradiation. Although this voltage is not high at present, we deduce that a 1 V voltage can be generated by integrated devices with an area of 0.01 m^2, which demonstrates the possibility of electricity generation from sunlight via the PTE effect. Further development of this work will aim at construction of large area and highly integrated device array toward their realistic applications.

In summary, we have demonstrated that poly[Cu_x(Cu-ett)]:PVDF is an excellent organic PTE composite. It should be emphasized that electrode/active-layer interface-located NIR irradiation and appropriate active-layer width are essential for the generation of a maximum V_{PTE} of up to 12 mV across a single device. More importantly, the photoexcitation of poly[Cu_x(Cu-ett)] enables an obvious increase in Seebeck coefficient from 52 ± 1.5 to 79 ± 5.0 μV/K, and thus provides a powerful strategy for the enhancement of the TE properties of organic materials. The prominent interface-located PTE effect of poly[Cu_x(Cu-ett)], makes photo to heat and heat to electric conversion in a single solution processed film, and allows for the sensitive detection of NIR light as well as electricity generation from solar energy.

■ ASSOCIATED CONTENT

Supporting Information

The detail information on devices fabrication; photothermoelectric properties and thermoelectric properties of different materials; molecular structure and SEM image of the organic thermoelectric materials; photothermoelectric properties of poly[Cu_x(Cu-ett)]:PVDF-based devices with vertical structure. This material is available free of charge via the Internet at http://pubs.acs.org.

■ AUTHOR INFORMATION

Corresponding Authors

*E-mail: dicha@iccas.ac.cn;.
*E-mail: wxu@iccas.ac.cn;.
*E-mail: zhudb@iccas.ac.cn.

Notes

The authors declare no competing financial interest.

■ ACKNOWLEDGMENTS

This research was financially supported by the Major State Basic Research Development Program (2013CB632500), the Strategic Priority Research Program of the Chinese Academy of Sciences (XDB12010000), and the National Natural Science Foundation (21422310, 61171055 and 21333011).

■ REFERENCES

(1) Choy, C. L. Thermal-Conductivity of Polymers. *Polymer* **1977**, *18*, 984–1004.
(2) Poehler, T. O.; Katz, H. E. Prospects for Polymer-Based Thermoelectrics: State of the Art And Theoretical Analysis. *Energy Environ. Sci.* **2012**, *5*, 8110–8115.
(3) Bubnova, O.; Crispin, X. Towards Polymer-Based Organic Thermoelectric Generators. *Energy Environ. Sci.* **2012**, *5*, 9345–9362.

DOI: 10.1021/acsami.5b01460
ACS Appl. Mater. Interfaces 2015, 7, 8968–8973

(4) Zhang, Q.; Sun, Y.; Xu, W.; Zhu, D. Organic Thermoelectric Materials: Emerging Green Energy Materials Converting Heat to Electricity Directly and Efficiently. *Adv. Mater.* **2014**, *26*, 6829−6851.
(5) Boulanger, C. Thermoelectric Material Electroplating: A Historical Review. *J. Electron. Mater.* **2010**, *39*, 1818−1827.
(6) Zhang, Q.; Sun, Y.; Xu, W.; Zhu, D. Thermoelectric Energy From Flexible P3HT Films Doped With A Ferric Salt Of Triflimide Anions. *Energy Environ. Sci.* **2012**, *5*, 9639−9644.
(7) Bubnova, O.; Khan, Z. U.; Malti, A.; Braun, S.; Fahlman, M.; Berggren, M.; Crispin, X. Optimization of the Thermoelectric Figure of Merit in The Conducting Polymer Poly (3, 4-ethylenedioxythiophene). *Nat. Mater.* **2011**, *10*, 429−433.
(8) Bubnova, O.; Berggren, M.; Crispin, X. Tuning the Thermoelectric Properties of Conducting Polymers in an Electrochemical Transistor. *J. Am. Chem. Soc.* **2012**, *134*, 16456−16459.
(9) Russ, B.; Robb, M. J.; Brunetti, F. G.; Miller, P. L.; Perry, E. E.; Patel, S. N.; Ho, V.; Chang, W. B.; Urban, J. J.; Chabinyc, M. L. Power Factor Enhancement in Solution-Processed Organic n-Type Thermoelectrics Through Molecular Design. *Adv. Mater.* **2014**, *26*, 3473−3477.
(10) Schlitz, R. A.; Brunetti, F. G.; Glaudell, A. M.; Miller, P. L.; Brady, M. A.; Takacs, C. J.; Hawker, C. J.; Chabinyc, M. L. Solubility-Limited Extrinsic n-Type Doping of a High Electron Mobility Polymer for Thermoelectric Applications. *Adv. Mater.* **2014**, *26*, 2825−2830.
(11) Sun, Y.; Sheng, P.; Di, C.; Jiao, F.; Xu, W.; Qiu, D.; Zhu, D. Organic Thermoelectric Materials and Devices Based on p-and n-Type Poly (metal 1,1,2,2-ethenetetrathiolate). *Adv. Mater.* **2012**, *24*, 932−937.
(12) Kim, G.; Shao, L.; Zhang, K.; Pipe, K. Engineered Doping of Organic Semiconductors for Enhanced Thermoelectric Efficiency. *Nat. Mater.* **2013**, *12*, 719−723.
(13) Kim, B.; Shin, H.; Park, T.; Lim, H.; Kim, E. NIR-Sensitive Poly (3, 4-ethylenedioxyselenophene) Derivatives for Transparent Photo-Thermo-Electric Converters. *Adv. Mater.* **2013**, *25*, 5483−5489.
(14) Xu, L.; Liu, Y.; Garrett, M. P.; Chen, B.; Hu, B. Enhancing Seebeck Effects by Using Excited States in Organic Semiconducting Polymer MEH-PPV Based on Multilayer Electrode/Polymer/Electrode Thin-Film Structure. *J. Phys. Chem. C* **2013**, *117*, 10264−10269.
(15) Basko, D. A Photothermoelectric Effect in Graphene. *Science* **2011**, *334*, 610−611.
(16) Gabor, N. M.; Song, J. C.; Ma, Q.; Nair, N. L.; Taychatanapat, T.; Watanabe, K.; Taniguchi, T.; Levitov, L. S.; Jarillo-Herrero, P. Hot Carrier−Assisted Intrinsic Photoresponse in Graphene. *Science* **2011**, *334*, 648−652.
(17) Song, J. C.; Rudner, M. S.; Marcus, C. M.; Levitov, L. S. Hot Carrier Transport And Photocurrent Response in Graphene. *Nano Lett.* **2011**, *11*, 4688−4692.
(18) Yan, K.; Wu, D.; Peng, H.; Jin, L.; Fu, Q.; Bao, X.; Liu, Z. Modulation-Doped Growth of Mosaic Graphene with Single-Crystalline p-n Junctions for Efficient Photocurrent Generation. *Nat. Commun.* **2012**, *3*, 1280−1286.
(19) Liu, C.-H.; Chang, Y.-C.; Norris, T. B.; Zhong, Z. Graphene Photodetectors with Ultra-Broadband And High Responsivity at Room Temperature. *Nat. Nanotechnol.* **2014**, *9*, 273−278.
(20) Sun, D.; Aivazian, G.; Jones, A. M.; Ross, J. S.; Yao, W.; Cobden, D.; Xu, X. Ultrafast Hot-Carrier-Dominated Photocurrent in Graphene. *Nat. Nanotechnol.* **2012**, *7*, 114−118.
(21) Wu, C.-C.; Jariwala, D.; Sangwan, V. K.; Marks, T. J.; Hersam, M. C.; Lauhon, L. J. Elucidating the photoresponse of Ultrathin MoS_2 Field-Effect Transistors by Scanning Photocurrent Microscopy. *J. Phys. Chem. Lett.* **2013**, *4*, 2508−2513.
(22) Wu, D.; Yan, K.; Zhou, Y.; Wang, H.; Lin, L.; Peng, H.; Liu, Z. Plasmon-Enhanced Photothermoelectric Conversion in Chemical Vapor Deposited Graphene p-n Junctions. *J. Am. Chem. Soc.* **2013**, *135*, 10926−10929.
(23) Jiao, F.; Di, C.-a.; Sun, Y.; Sheng, P.; Xu, W.; Zhu, D. Inkjet-Printed Flexible Organic Thin-Film Thermoelectric Devices Based On P-And N-Type Poly (Metal 1,1,2, 2-Ethenetetrathiolate) S/Polymer Composites Through Ball-Milling. *Philos. Trans. R. Soc London, Ser.. A* **2014**, *372*, 20130008.
(24) Iwamura, M.; Watanabe, H.; Ishii, K.; Takeuchi, S.; Tahara, T. Coherent Nuclear Dynamics in Ultrafast Photoinduced Structural Change of Bis(diimine)copper(I) Complex. *J. Am. Chem. Soc.* **2011**, *133*, 7728−7736.
(25) Tromp, M.; Dent, A. J.; Headspith, J.; Easun, T. L.; Sun, X.-Z.; George, M. W.; Mathon, O.; Smolentsev, G.; Hamilton, M. L.; Evans, J. Energy Dispersive XAFS: Characterization of Electronically Excited States of Copper(I) Complexes. *J. Phys. Chem. B* **2013**, *117*, 7381−7387.
(26) Fritzsche, H. A General Expression for the Thermoelectric Power. *Solid State Commun.* **1971**, *9*, 1813−1815.
(27) Pernstich, K. P.; Roessner, B.; Batlogg, B. Field-Effect-Modulated Seebeck Coefficient in Organic Semiconductors. *Nat. Mater.* **2008**, *7*, 321−325.
(28) Bubnova, O.; Khan, Z. U.; Wang, H.; Braun, S.; Evans, D. R.; Fabretto, M.; Hojati-Talemi, P.; Dagnelund, D.; Arlin, J.-B.; Geerts, Y. H.; Desbief, S.; Breiby, D. W.; Andreasen, J. W.; Lazzaroni, R.; Chen, W. M.; Zozoulenko, I.; Fahlman, M.; Murphy, P. J.; Berggren, M.; Crispin, X. Semi-Metallic Polymers. *Nat. Mater.* **2014**, *13*, 190−194.
(29) Buscema, M.; Barkelid, M.; Zwiller, V.; van der Zant, H. S.; Steele, G. A.; Castellanos-Gomez, A. Large and Tunable Photothermoelectric Effect in Single-layer MoS_2. *Nano Lett.* **2013**, *13*, 358−363.

DOI: 10.1021/acsami.5b01460
ACS Appl. Mater. Interfaces 2015, 7, 8968−8973